Mechanism Elucidation of Immune System ~ Using Chemicalbiological Method ~

Contents

1. Introduction

1-1. Mechanism of Immune System

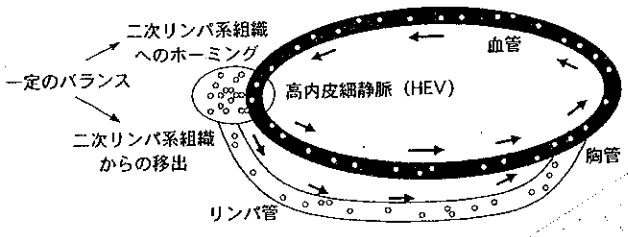

Fig.1-1 Lymphocyte is circulating through blood vessel and lymphatic around body once a day, and watching over not to be invaded by virus and so on.

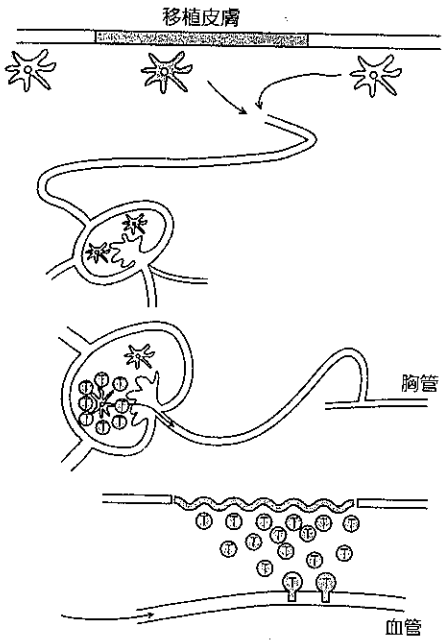

Fig.1-2

The dendritic cells find the invader such as virus or transplanted organ, these cells move to lymph node to inform the invasion to lymphocytes.

Based on the information from dendritic cells, T-cells are activated and starts to proliferate in the lymph node.

The proliferated T-Lymphocytes are moving to the invaded sites and kill the invaders.

1-2. Recognition of Self and Non-self cells

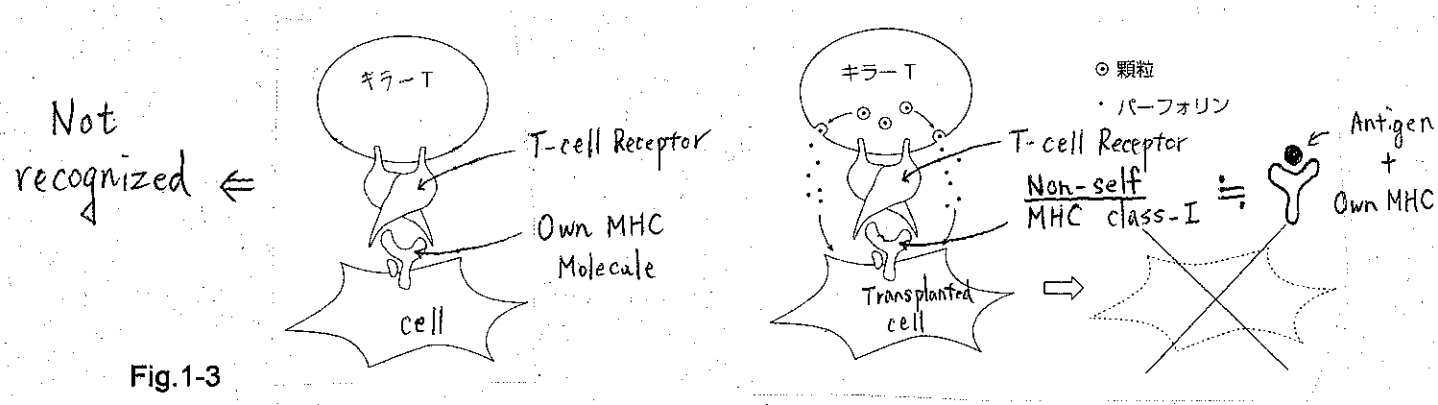

Fig.1-3

Transplanted organs are also recognized as an antigen and removed by Cytotoxic T-Lymphocytes. This rejection is the problem in regard to transplantation.

It is necessary to develop immunosuppressive agent

2. Development of Immunology with FK 506

2-1. Immunophilin* Ligands

(*Imuunophilin; immunosuppressant binding protein)

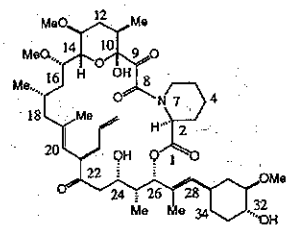

FK506

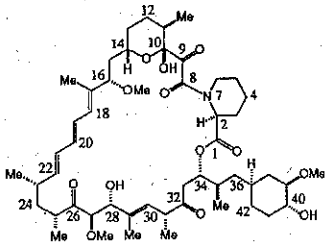

Rapamycin

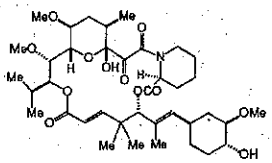

506BD

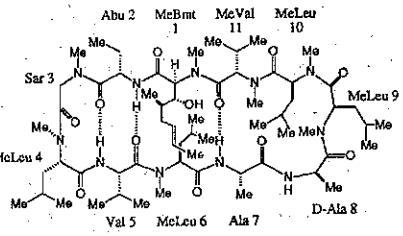

Cyclosporin A (CsA)

FKBP
(FK506 binding protein)

CyP
(Cyclosporin A binding protein)

FK506 (Prograf) was found to be strong immunosuppressive agent !!

2-2. Elucidation of Immune Response System Using FK506 and its Derivatives

2-2-1. How to Purify FKBP and CyP

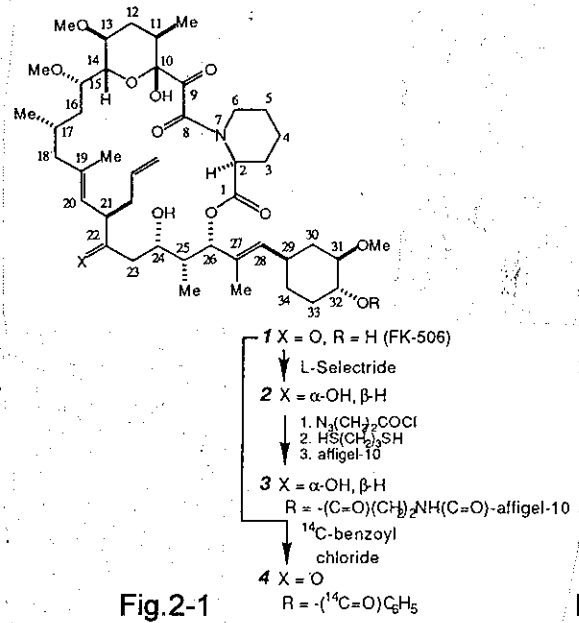

Fig.2-1
The synthesis of FK506 Affinity Gel

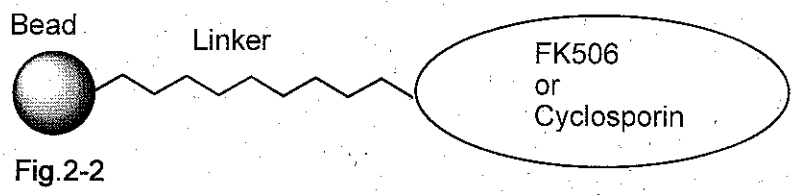

Fig.2-2

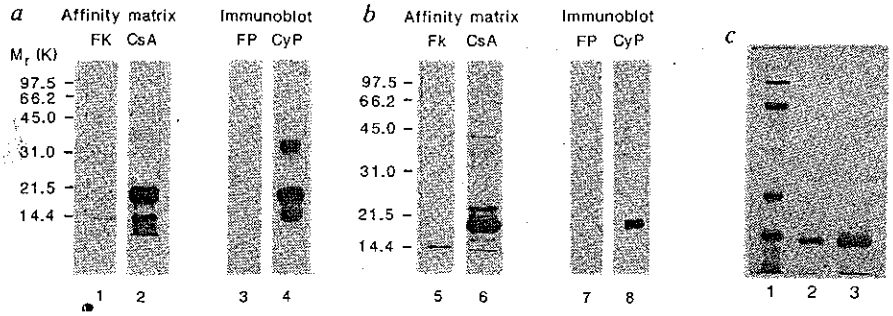

Fig.2-3 The Purification of FKBP and CyP Using SDS-PAGE
It was determined that FKBP was approximately14 kD and CyP was approximately 20 kD.

2-2-2. Rotamase Activity of FK506 Binding Protein (FKBP) and Cyclosporin A binding protein (CyP)

Stuart L. Schreiber. et al, *Nature,* 1989. *341*, 758.

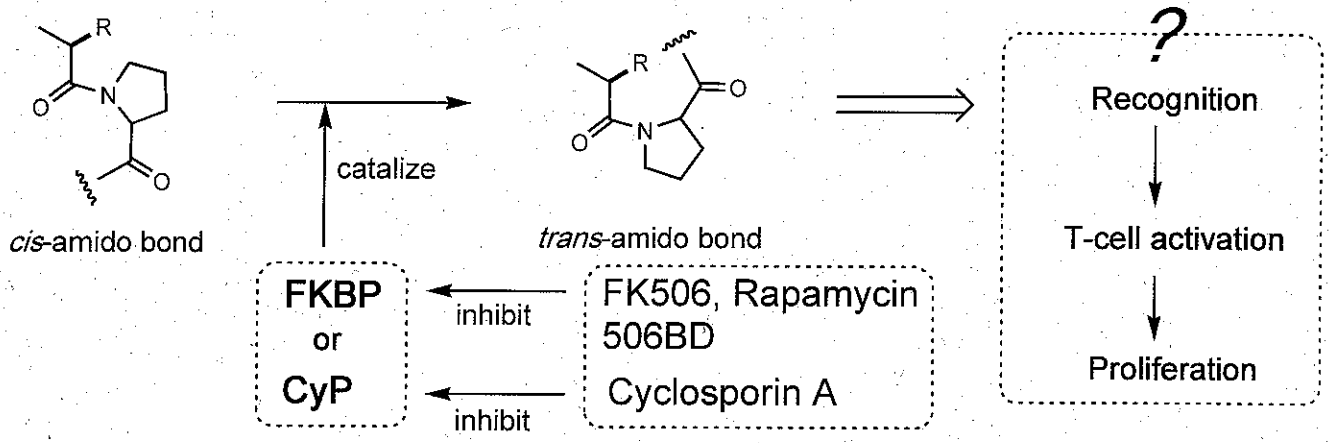

2-2-3. Denial of Relationship Between Rotamase Activity and T-Cell Proliferation

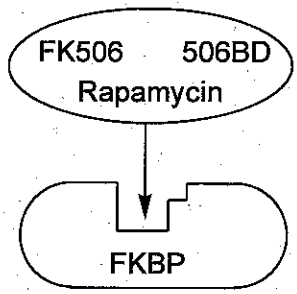

FK506, Rapamycin, and 506BD which is synthetic FKBP ligand, interact with a common domain of FKBP through their common structural elements by NMR and crystallographic study.

S. L. Schreiber, *J. Am. Chem. Soc.* 1991, *113*, 2339.

And these compound inhibit the rotamase activity of FKBP.

⇓

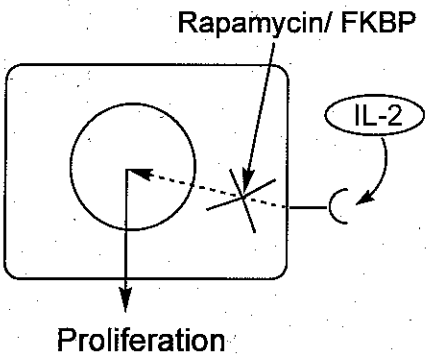

But...

Rapamycin does not inhibit the same TCR-mediated signaling pathway that is affected by FK506 and CsA. Rather, it blocks a later Ca^{2+}-independent pathway associated with T-cell activation, which is mediated by the IL-2 receptor.

And 506BD has **no inhibitory effect** on either of the signaling pathways inhibited by FK506 or rapamycin.

⇓

Suggestion

Not eliminating the function of FKBP
Adding the function to FKBP

"Active complex"

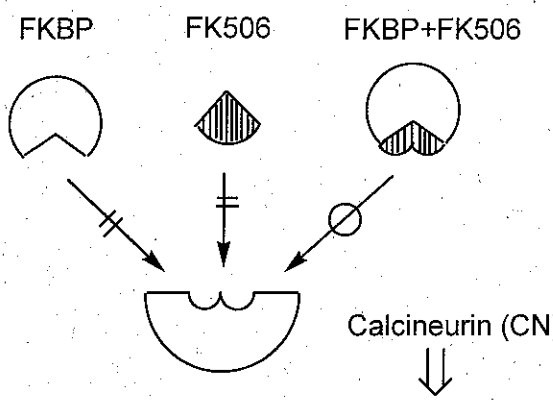

Calcineurin (CN)

⇓

Carmodurin dependent
Serin/Threonine protein phosphatase

⇒ Inhibited by FKBP-FK506 or CyP-CsA

(mesured with phosphopeptide substrate)

S. L. Schreiber, *Cell.* 1991, *66*, 807.

NFAT-P
(Nucleus Factor of Activated T-Cell)

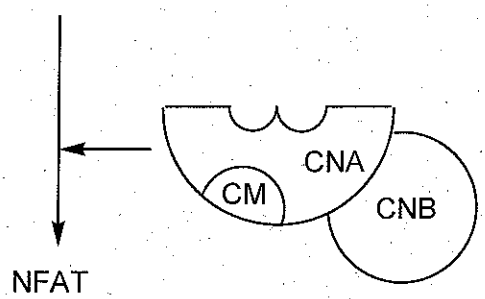

NFAT

Fig.2-4 Structure CN and its activity

CM= Carmodulin
(It binds to calcium ion and then activates CN.)

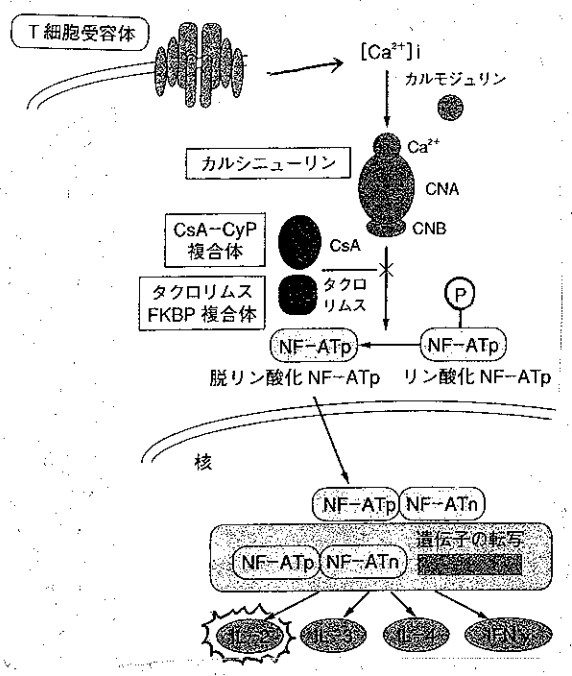

Fig.2-5 Summary of Immune System in regard to FK506 and CsA

3. Discovery of Novel Immunosuppressant, Myriocin

Trichoderma

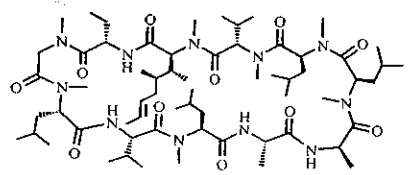

シクロスポリン A (CsA)

IC_{50}= 27 nM

Coproduct from *Trichoderma*

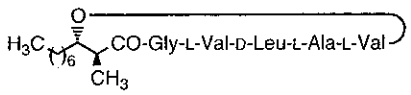

トリコスポリド（トリコデルマ属菌より単離）

Isaria

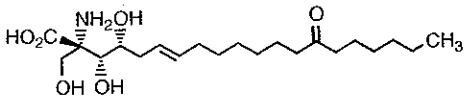

ミリオシン（イサリア属菌より単離）

IC_{50}= 3.0 nM

Screening using MLR*

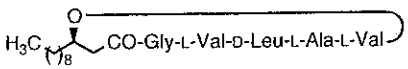

イサリイン（イサリア属菌より単離）

MLR*= Mixed Lymphocyte Reaction

(a) 混合リンパ球反応（MLR）

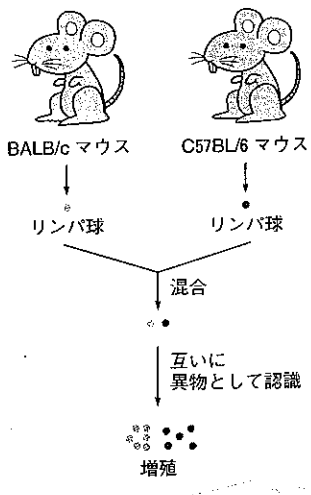

(b) スクリーニング系

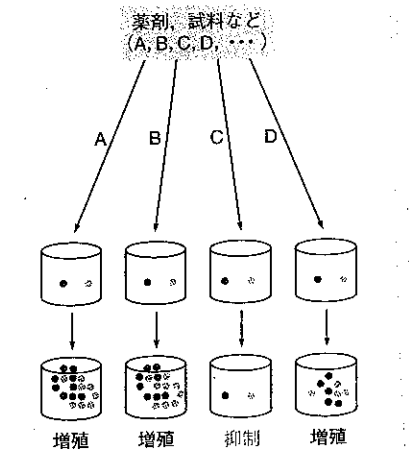

試料 C が免疫抑制作用を有すると考えられる

It is required that the results *in vitro* reflect correctly the results *in vivo*.
At this poin, MLR screening is excellent method.

Myriocine has hydrophilic zwitter ion and lipophilic alkyl chain.
It induces insolubility and toxicity to this molecule.

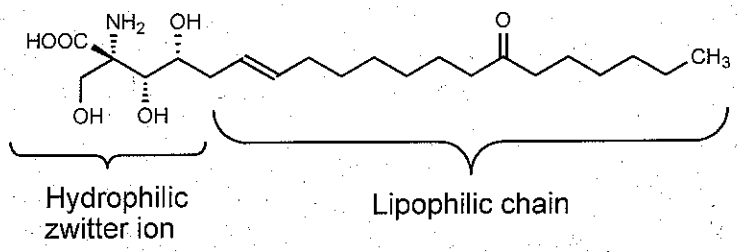

4. Total Synthesis of Myriocin

Myriocine has tree stereo centers including one quaternary carbon atom.
Synthesis of α-substituted serine is interesting.

N. Chida, *Chem. Commun.*, 2001, 1932

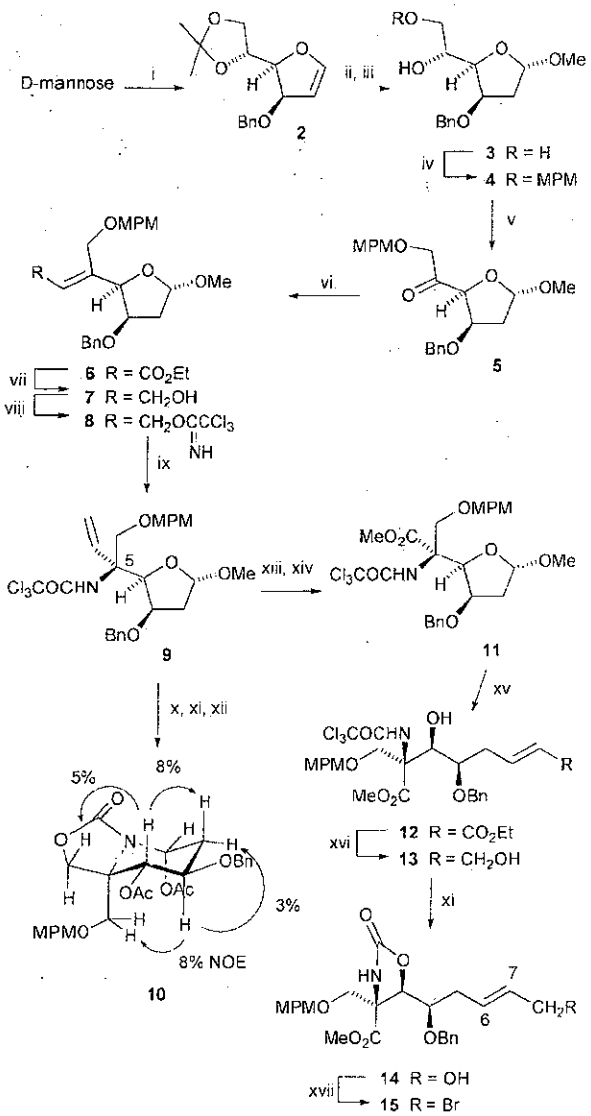

Scheme 1 Bn = $-CH_2Ph$, MPM = $-CH_2C_6H_4$-*p*-OMe. *Reagents and conditions*: i see ref. 9; ii $Hg(OAc)_2$, THF–H_2O, room temp., then KI, $NaBH_4$, THF–H_2O, 0 °C; iii AcOH–H_2O (3:2), room temp., then AcCl, MeOH, 0 °C; iv *n*-Bu_2SnO, toluene, reflux, then MPMCl, CsF, DMF, 70 °C; v $(COCl)_2$, DMSO, CH_2Cl_2, −78 °C, then Et_3N, 0 °C; vi $(MeO)_2P(O)CH_2CO_2Me$, LiBr, DBU, CH_3CN, −40 °C; vii DIBAL-H, toluene, −78 °C; viii Cl_3CCN, DBU, CH_2Cl_2, 0 °C; ix K_2CO_3, *o*-xylene, 140 °C; x O_3, MeOH, −78 °C, then $NaBH_4$, 0 °C; xi DBU, CH_2Cl_2, room temp.; xii 1 M aqueous HCl–THF (1:1), room temp., then Ac_2O, DMAP, pyridine, room temp.; xiii O_3, CH_2Cl_2, −78 °C, then Me_2S; xiv $NaClO_2$, NaH_2PO_4, $HOSO_2NH_2$, t-BuOH–H_2O, room temp., then Me_3SiCHN_2, MeOH, room temp.; xv 4 M aqueous HCl–THF (1:3), room temp., then $Ph_3P{=}CHCO_2Et$, toluene, room temp.; xvi DIBAL-H, THF–toluene, −15 °C; xvii MsCl, Et_3N, CH_2Cl_2, 0 °C, then LiBr, acetone, room temp.

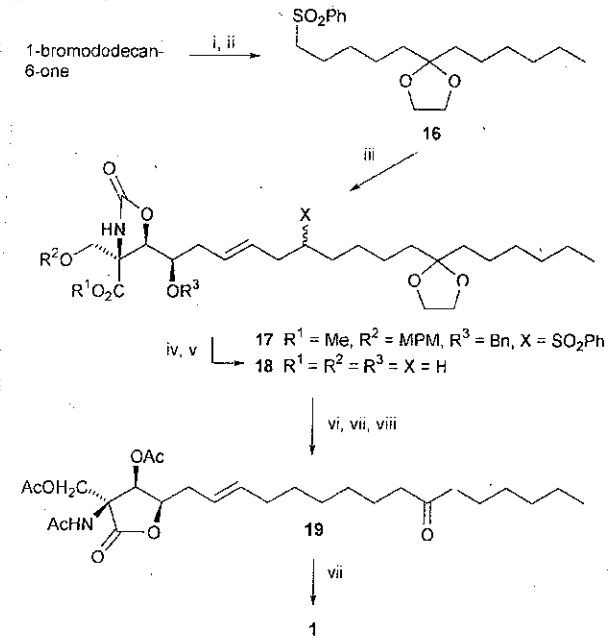

Scheme 2 *Reagents and conditions*: i $PhSO_2Na$, DMF, room temp.; ii $(TMSOCH_2)_2$, TMSOTf, CH_2Cl_2, room temp.; iii *n*-BuLi, THF, −78 °C, then **15**, −78–0 °C; iv LiOH, H_2O–MeOH, room temp.; v Li, liq. NH_3, THF, −78 °C; vi 4 M aqueous HCl–THF (1:1), room temp.; vii 10% aqueous NaOH–MeOH (1:3), reflux; viii Ac_2O, pyridine, room temp.

Scheme 1 ii Oxymercuration.

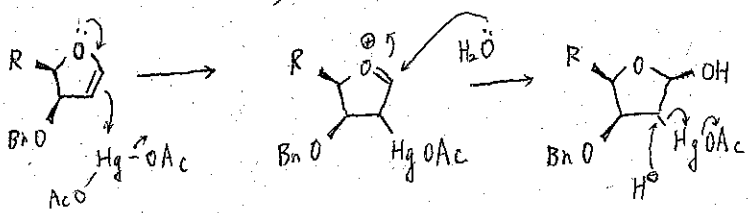

$NaBH_4$ → − Hg, − OAc

Markovnikov rule.

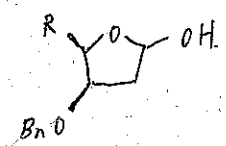

ix Overman rearrangement.

Mechanism of the thermal rearrangement:

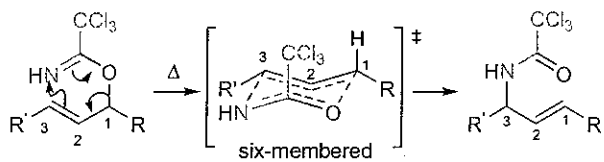

iv Selective protection of primary alcohol using tin-acetal.

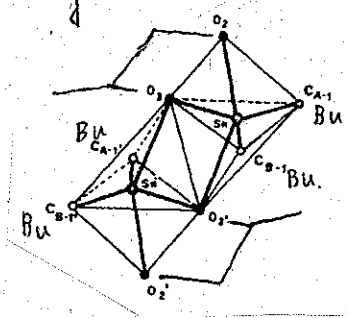

compound 8

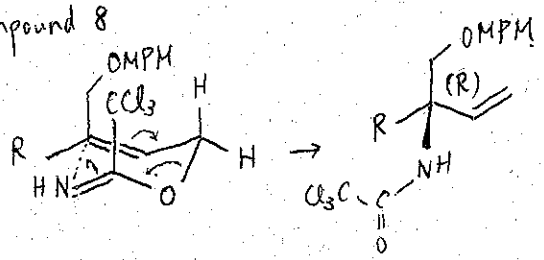

5. Elucidation of Activities of Myriocin

5-1. Serine Palmitoyl Transferase (SPT) Inhibitor

T. Kawasaki, *Biochem. Biophys. Res. Commun.* 1995, *211*, 396.

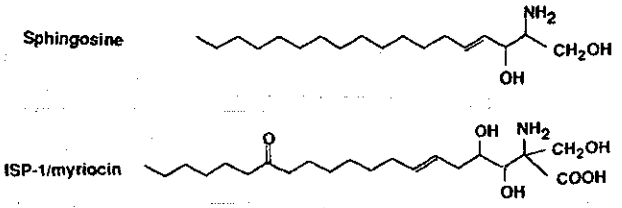

⇒ It was suggested that Myriocin had some relations to sphingolipid biosynthesis.

Fig. 5-1 Similarity Between Sphingosine and Myriocin

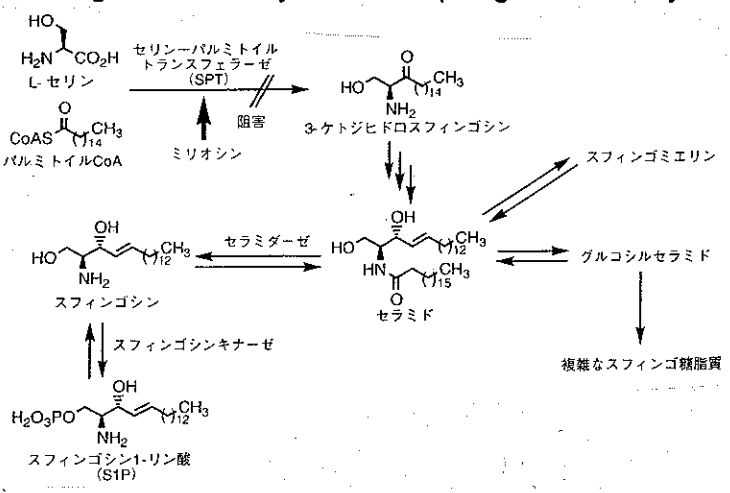

Fig. 5-2 Biosynthesis Pathway of Sphingolipid

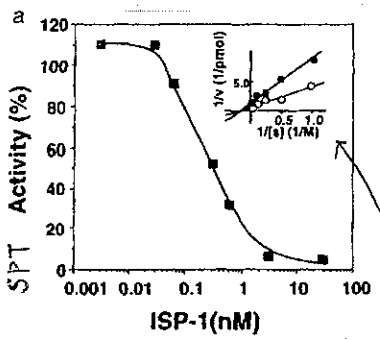

V_{Max} change means Non-Competitive Inhibition

Fig. 5-3 Lineweaver-Burk Plots

Kinetic data of SPT with or without myriocin.

⇓

It is suggested that SPT inhibition should prevent T-cell from proliferating.

Table 5-1 Growth Recovery after Various Treatments

Table I. Growth Recovery after Various Treatments

Effector	% Recovery [a]
Sphingosine	97
Sphingosine-1-phosphate	120
DL-*erythro, threo*-Dihydrosphingosine	42
DL-*erythro*-Dihydrosphingosine	59
DL-*threo*-Dihydrosphingosine	7
Dimethylsphingosine	0
Ceramide	0
C2-ceramide	13
Sphingomyelin	0
Sphingomyelinase	32
Galactosylceramide	0
Glucosylceramide	0
GM3	0
Sphingosine +Fumonisin B1	87

1. Sphingosin and Sphingosine-1-phosphate has a great ability to restore the proliferation.
2. Ceramide has no ability to restore the proliferation. But C2-ceramide has a little ability due to its permeability.
3. Sphingomyeline and glicosphingolipid has no ability to restore the proliferation.

⇓

The inhibition of T-cell proliferation is derived from the depletion of Sphingosine and Sphingosine-1-phosphate and ceramide.

The recovering ability of ceramide is weaker than that of sphingosine-1-phosphate.

Fumonisin B1, which is a potent inhibitor of sphingosine N-acyltransferase and inhibits the conversion of sphingosine to ceramide, did not significantly suppress the effects of sphingosine.

⇓

Recently it is shown that Sphingosine-1-phosphate is involved in the PDGF pathway.

PDFG (Platelet-Derived Growth Factor) activated Sphingosine kinase and induced cell proliferation.

S.Spiegel, *Nature.* 1993, *365*, 557.

5-2. Identification of Myriocin-Binding Proteins

S. L. Schreiber, *Chem&Biol.*1999, *6*, 221.

Direct relationship between inhibition of SPT and immunosuppresion is not elucidated.

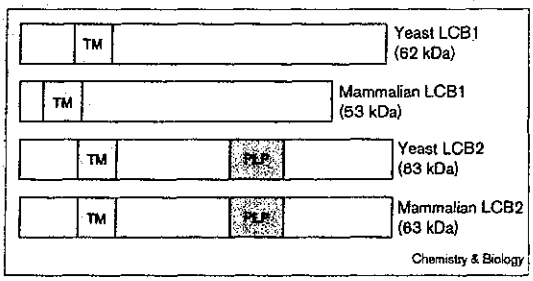

Schematic representation of the yeast and mammalian LCB proteins. Putative transmembrane (TM) and PLP-binding regions (PLP) are shown.

Fig. 5-4 LCB proteins.

LCB1 and LCB2 is putative SPT subunit.

Two genes that encode putative SPT subunits was identified.

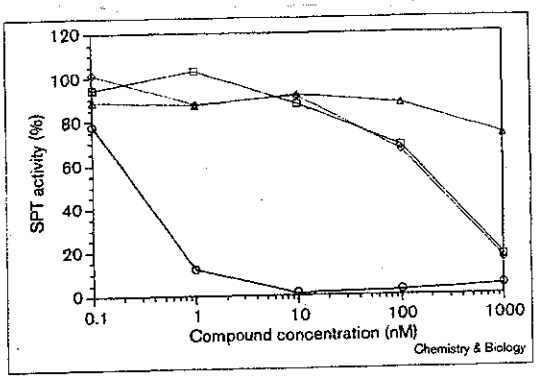

Inhibition of CTLL-2 microsomal serine palmitoyltransferase activity by myriocin (**1**, black circles), C20-linker myriocin (**4**, red triangles), *N*-linker myriocin (**16**, blue squares), and C1-linker myriocin (**21**, green diamonds).

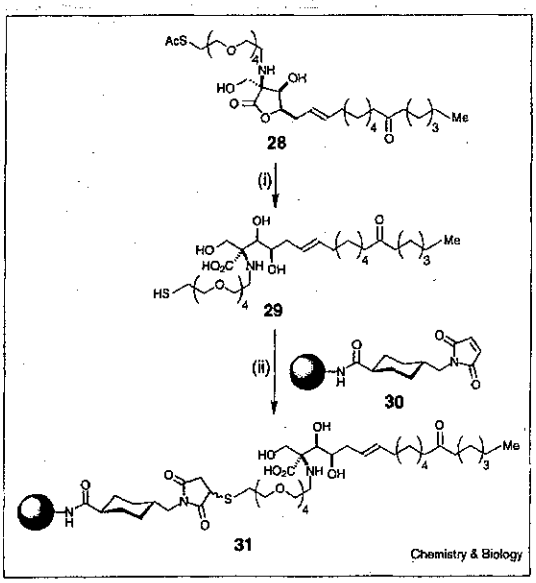

Synthesis of N-linker myriocin affinity matrix. **(i)** LiOH(aq), THF/MeOH, 0°C, 60%; **(ii)** TCEP, MeOH/PBS (pH 7.4), rt, 100%.

Fig. 5-6

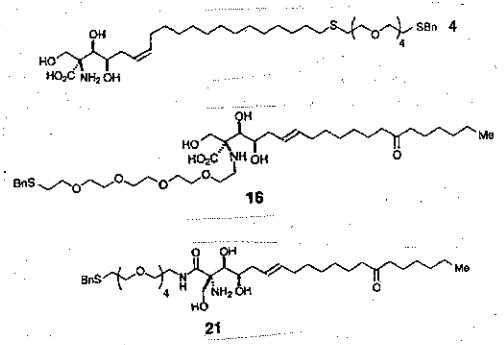

⇒ C-20 linker.

⇒ N-linker

⇒ C1-linker

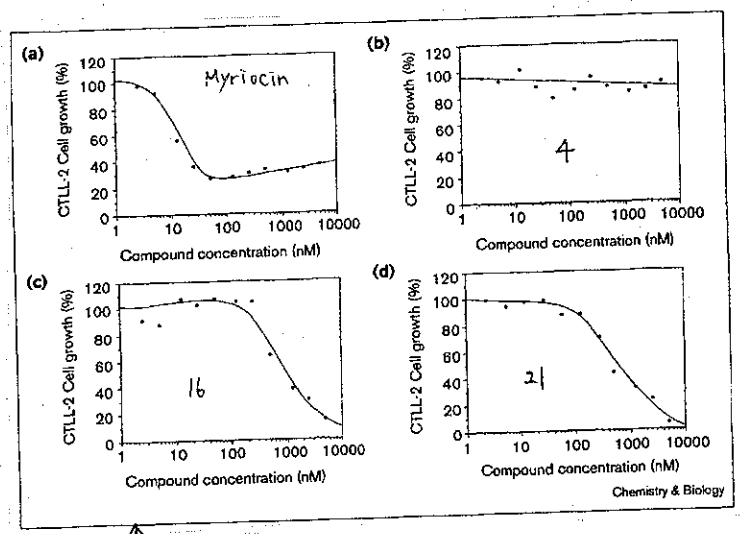

Fig. 5-5

Inhibition of CTLL-2 cell growth by **(a)** myriocin and its derivatives, **(b)** C-20 linker myriocin **4**, **(c)** N-linker myriocin **16** and **(d)** C1-linker myriocin **21**.

in vivo

in vitro

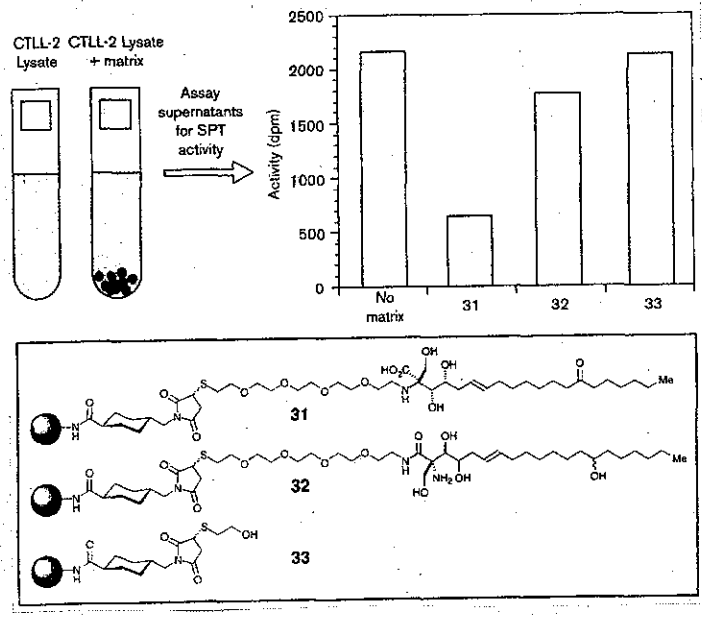

Fig. 5-7

Binding of factors comprising serine palmitoyltransferase activity by myriocin-containing matrices.

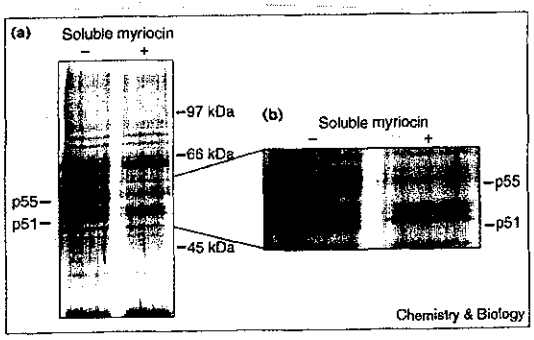

Detergent-solubilized proteins from CTLL-2 microsomes that bind to the *N*-linker myriocin matrix (31). **(a)** Complete range of matrix-associated proteins. **(b)** Close-up view of the 50–60 kDa region. Specific myriocin-binding proteins p51 and p55 do not associate with the affinity matrix in the presence of soluble myriocin. (The 60 kDa protein in this gel that appears to be able to compete with myriocin is nonreproducible and was not characterized further).

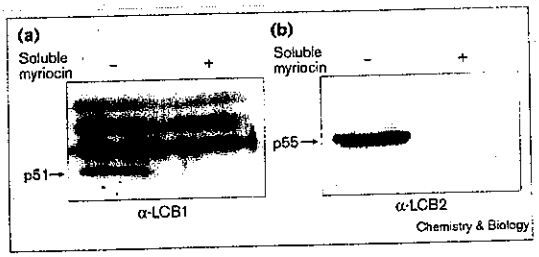

Western blot analyses of affinity matrix-associated proteins. **(a)** Recognition of specific myriocin-binding protein p51 by an α-LCB1 antibody. Cross-reactive proteins bind to the matrix nonspecifically and are also recognized by preimmune sera (data not shown). **(b)** Recognition of specific myriocin-binding protein p55 by an α-LCB2 antibody. Neither p51 or p55 is recognized by preimmune sera.

Fig.5-8

p51 and p55 is specific myriocin-binding protein.

Fig.5-9

Western blot using the antibody derived from LCB1 and LCB2.
p51 binds to the antibody derived from LCB1.
p55 binds to the antibody derived from LCB2.

It is strongly suggested that p51 is LCB1 and p55 is LCB2.

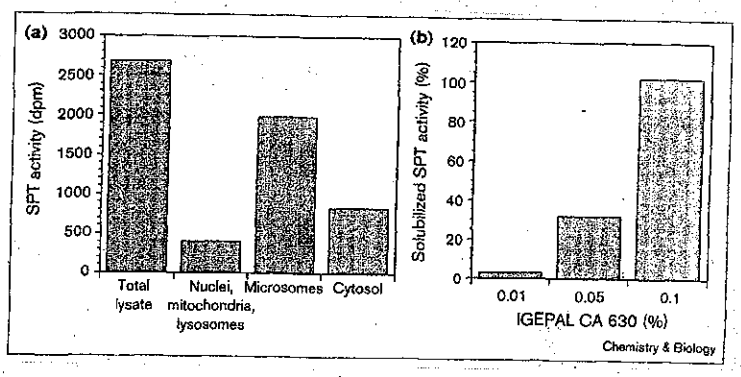

Fig. 5-10 Subcellular localization of SPT activity.

(a) SPT activity in various lysate fractions obtained by differential centrafugation.

(b) Solubilization of microsomal SPT activity by IGEPAL CA 630.

This result also supports that suggestion shown above.

5-3. Acceptable mechanism of 3-ketodihidrosphingosine biosynthesis

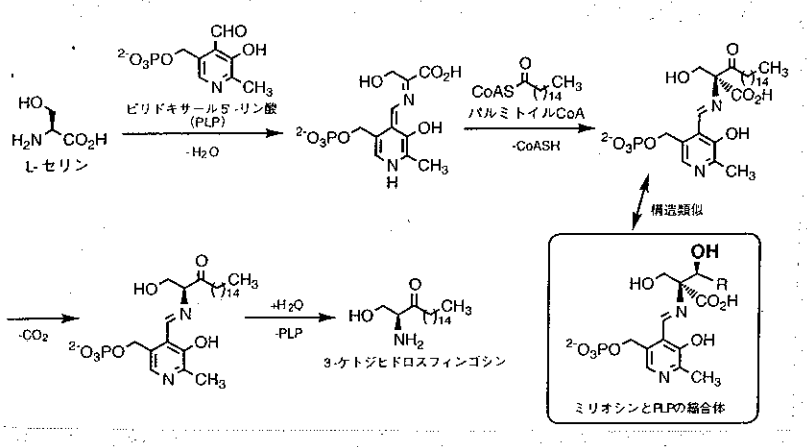

6. Discovery of FTY720

化合物構造	化合物名	免疫抑制活性 MLR, IC_{50} (nM)
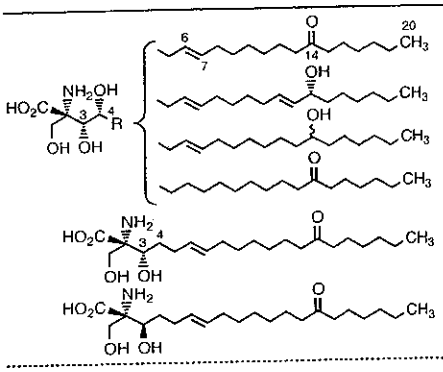	ミリオシン	3.0
	ミセステリシンA	8.9
	ミセステリシンB	2.5
	ミセステリシンC	6.2
	ミセステリシンD	16
	ミセステリシンE	13
	CsA	14

Fig. 6-1. Analogues of Myriocin.
These compounds were isolated from.
Mycelia sterilia.

化合物構造	化合物名	免疫抑制活性 MLR, IC_{50} (nM)
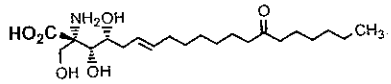	ミリオシン	3.0
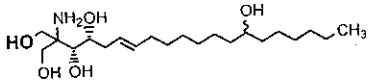		4.7
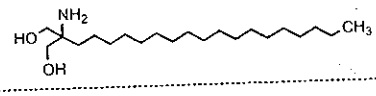		12
	CsA	14

Fig. 6-2. Simplification of Myriocine
Aim at.
① reducing its toxicity.
② improving its physicochemical properties
③ identifying the structure essential for immunosuppressive activity.

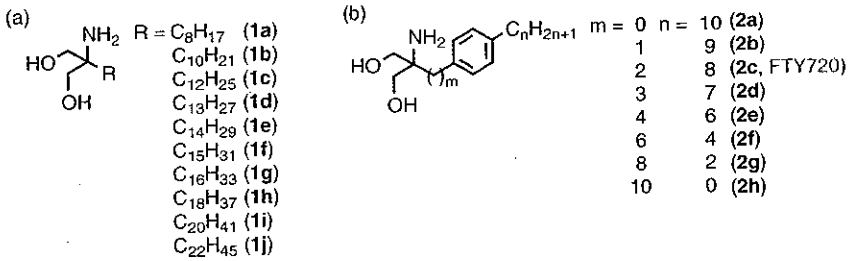

図15・7 (a)側鎖長の異なる2-アミノプロパン-1,3-ジオール．(b)側鎖長を一定にし，フェニル基を移動させた2-アミノプロパン-1,3-ジオール．

表15・1 一連の2-アミノプロパン-1,3-ジオール骨格を有する化合物のMLRにおける抑制作用．側鎖長とベンゼン環の位置は，活性に重要である．化合物**2c**が臨床試験中のFTY720である

化合物番号 (図15・7a)	免疫抑制活性 MLR, IC_{50} (nM)	化合物番号 (図15・7b)	免疫抑制活性 MLR, IC_{50} (nM)
1a	3700	**2a**	13
1b	440	**2b**	70
1c	270	**2c (FTY720)**	6.1
1d	12	**2d**	350
1e	5.9	**2e**	19
1f	2.9	**2f**	100
1g	10	**2g**	32
1h	12	**2h**	54
1i	190		
1i	1600		

Fig. 6-3 Further conversion.

7. Elucidation of Activities of FTY720

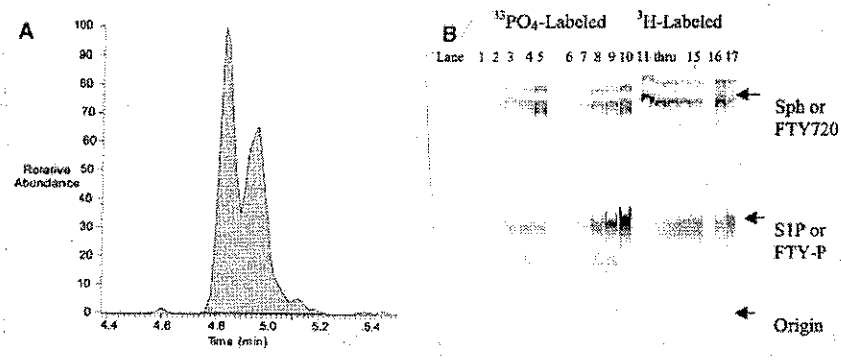

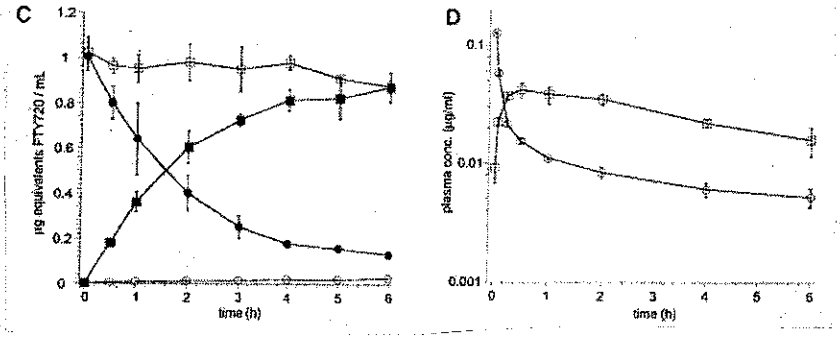

Metabolism of FTY720 analyzed by LCMS. (**A**) FTY720 and a +80d adduct were found in mouse plasma after IV dosing with FTY720. (**B**) Phosphorimager thin-layer chromatography scan showed incorporation of $^{33}PO_4$ in FTY720 by incubation in whole rat blood: vehicle (lanes 1 to 5) and 25 μM FTY720 (lanes 6 to 10) at 0, 0.5, 2, 4, or 18 hours; rat blood with ^{3}H-FTY720 at 0, 1, 2, 4, or 18 hours (lanes 11 to 15) or ^{3}H-sphingosine at 30 and 60 min (lanes 16 and 17). Arrows indicate standards. (**C**) Compound A*(■) was generated from FTY720 (●) by in vitro incubation of rat blood. Synthetic Compound A (□) was not converted to FTY720 (○). (**D**) FTY720 (○) was converted to Compound A (□) faster in rats (0.5 mg/kg IV) than in blood ex vivo. The steady-state ratio at 1 hour indicated dephosphorylation outside blood. See (7) for experimental details.

Fig. 7-1 Metabolism of FTY720.

* Compound A is FTY720-Phosphonate.

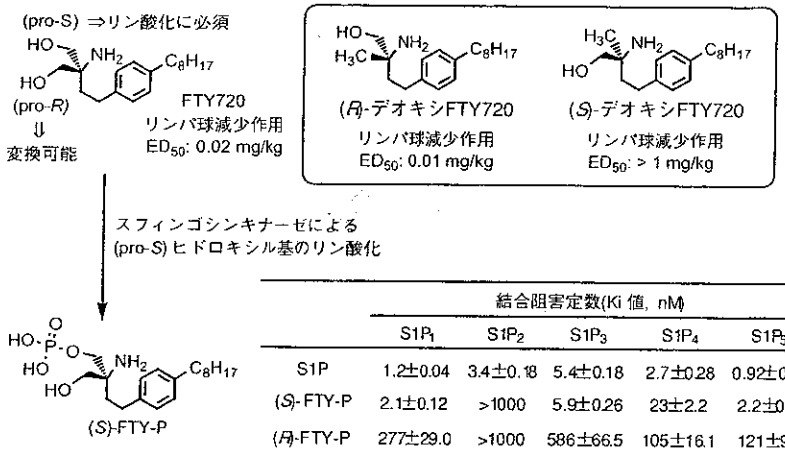

	結合阻害定数(Ki 値, nM)				
	$S1P_1$	$S1P_2$	$S1P_3$	$S1P_4$	$S1P_5$
S1P	1.2±0.04	3.4±0.18	5.4±0.18	2.7±0.28	0.92±0.18
(S)-FTY-P	2.1±0.12	>1000	5.9±0.26	23±2.2	2.2±0.25
(R)-FTY-P	277±29.0	>1000	586±66.5	105±16.1	121±9.5

Fig. 7-4 Enantioselective phosphorylation.

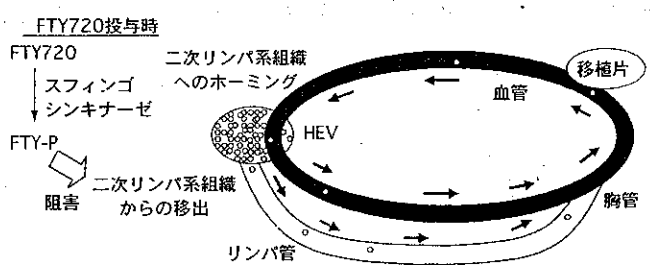

Fig. 7-2. Effect of FTY720.

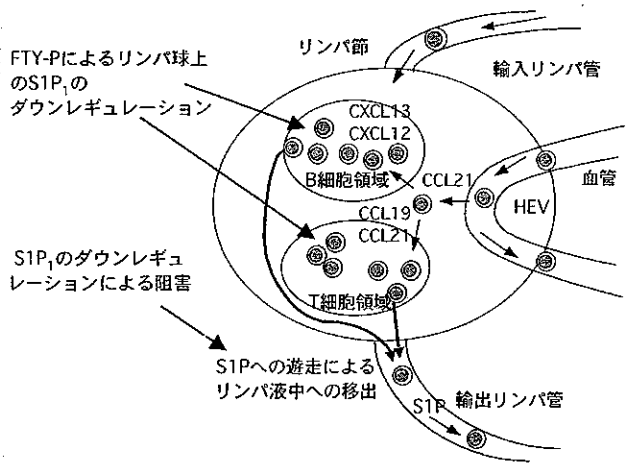

Fig. 7-3. Mechanism of Sequestering Lymphocytes into Lymph node

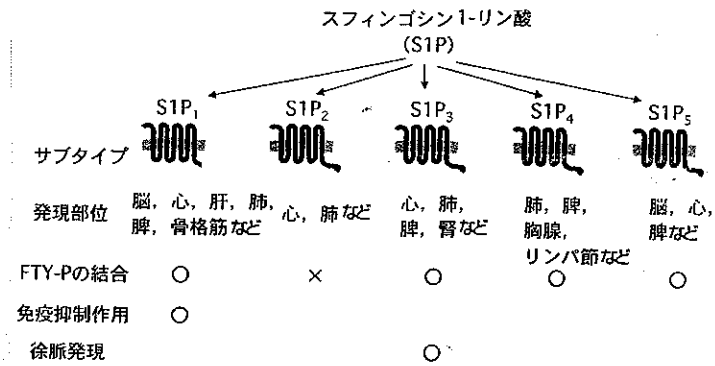

Fig. 7-5 Subtypes of S1PR

$S1P_3$ has relation to acute bradycardia. Acute bradycardia is the side effect of FTY720.

Further Investigation to conquest the side effect of FTY720

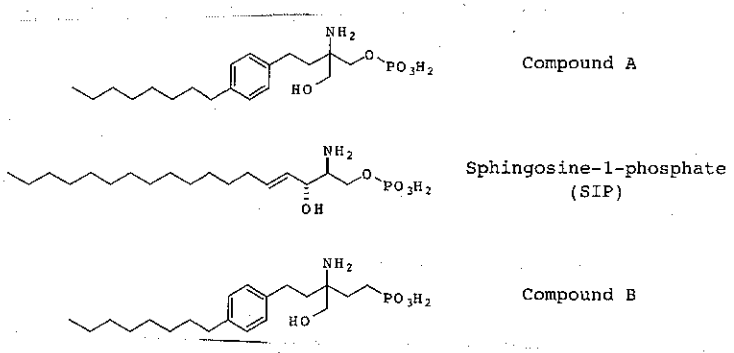

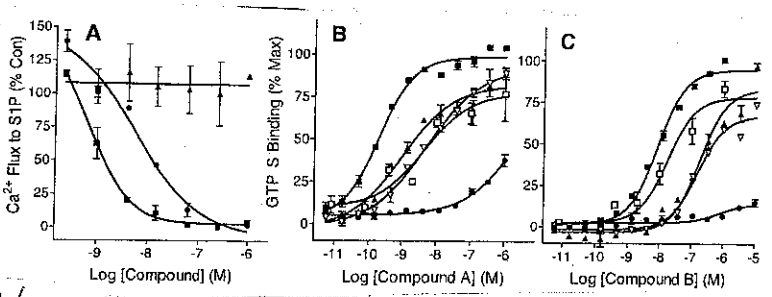

Fig. 7-6 Agonist activity of compounds (7). (A) HUVEC were pretreated with Compound A (■), S1P (●) or FTY720 (▲) for 10 min and Ca^{++} flux in response to 200 nM sphingosine-1-phosphate was measured (n = 3). (B, C) ^{35}S-GTPγS binding was measured in transfected CHO cells expressing $S1P_1$ (■) $S1P_2$ (●), $S1P_3$ (△), $S1P_4$ (□), and $S1P_5$ (▲) receptors in response to Compound A (B) or Compound B (C). EC_{50} values (nM) were 0.2, >1000, 4.9, 4.3 and 1.0 for Compound A, and 8.2, >10,000, 151, 33, and 178 for compound B on $S1P_1$, $S1P_2$, $S1P_3$, $S1P_4$, and $S1P_5$, respectively (n = 3). See (7) for experimental details.

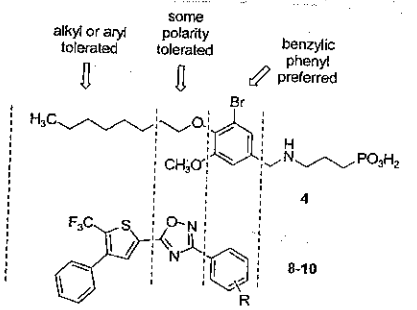

Figure 1. SAR summary and rationale for HTS lead utilization.

Table 2. S1P Receptor Affinities (IC_{50}, nM)[a] for "HTS Side Chain" Analogues

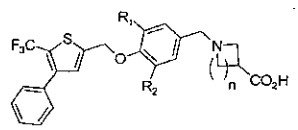

compd	n	R_1	R_2	$S1P_1$	$S1P_3$	$S1P_4$	$S1P_5$
S1P				0.67	0.26	34	0.55
2				0.28	6.3	15	0.77
15				8.3[b]	1000[c]	10000	16
18	1	H	H	1.2	530	1600	23
19[d]	2	H	H	4.3	1000	790	120
20	1	CF_3	H	7.7	>10000	340	21
21	1	Br	H	13	>10000	2400	53
22	1	Cl	H	3.2	2000	1300	18
23	1	F	H	2.7	2100	2700	41
24	1	CH_3	H	1.8	7500	1500	13
25	1	CH_2CH_3	H	3.5	4300	>10000	10
26	1	OCH_3	H	33	>10000	2800	77
27	1	CH_3	CH_3	4.0	10000	120	12
28	1	Cl	Cl	7.5	>10000	640	33

[a] Displacement of [^{33}P]-labeled sphingosine-1-phosphate (S1P) by test compounds from human S1P receptors expressed on CHO cell membranes. Data are reported as mean for n = 3 determinations. SD were generally ± 20% of the average. All new compounds had $S1P_2$ IC_{50} >10000 nM. See ref 7b for assay protocol. [b] EC_{50} = 0.2 nM. [c] EC_{50} = 17 nM. [d] Racemate.

Fig. 7-8

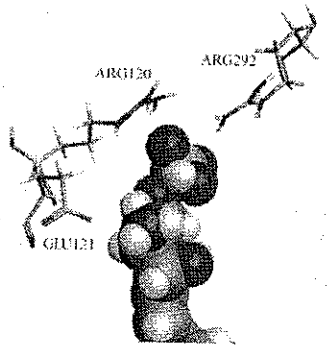

Fig. 7-7
S1P - S1PR binding model

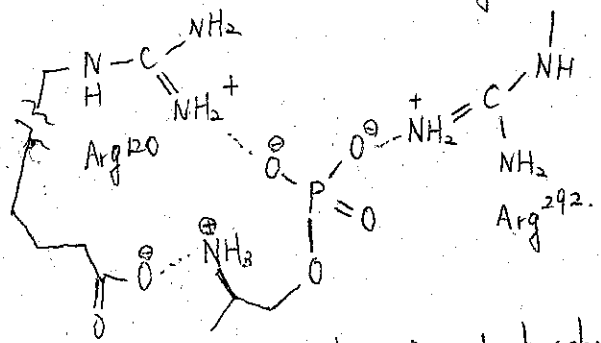

This binding pocket is found in $S1P_1$, $S1P_3$, $S1P_4$, $S1P_5$.

Change the phosphonate into other acid moiety.

The selectivity against $S1P_3$ is greatly improved!